in C–Ti–C angle to 75.8°. Minimal changes occurred in the remaining angles and distances. The total energy for the complex was reduced by only 4.2 kcal/mol as a result of this further optimization.[38] This final geometry is shown in Figure 1A.

D. Form of the Transition-State Wave Function. The wave function superposition represented in eq 7 appears in terms of Young tableau[39] as

$$\psi(\text{TS})_+ = \boxed{\begin{array}{cc} \pi_2 & \pi_3 \\ \pi_1 & \pi_4 \end{array}} + \boxed{\begin{array}{cc} \pi_1 & \pi_2 \\ \pi_3 & \pi_4 \end{array}} = \boxed{\begin{array}{cc} \pi_1 & \pi_2 \\ \pi_3 & \pi_4 \end{array}} \quad (A2)$$

Because orbital pairs $\pi_1-\pi_3$ and $\pi_2-\pi_4$ are triplet coupled here, they may be taken as orthogonal without restriction (the antisymmetrizer projects away any nonorthogonalities). The total wave function has an overall singlet spin coupling, and a more complete representation of the transition state must include the remaining linearly independent singlet coupling of these orthogonal orbitals[11g]

(38) Total energies from configuration interaction calculations are as follows: metallacycle, −1884.0677; π complex, −1884.0534; transition state, −1884.0498; alkylidene + olefin, −1884.0344.

(39) See, for example: Pauncz, R. "Spin Eigenfunctions, Construction and Use"; Plenum Press: New York, 1979.

$$\psi(\text{TS})_+ = \lambda_1 \boxed{\begin{array}{cc} \pi_1 & \pi_2 \\ \pi_3 & \pi_4 \end{array}} + \lambda_2 \boxed{\begin{array}{cc} \pi_1 & \pi_3 \\ \pi_2 & \pi_4 \end{array}} = \lambda_1 \phi_+^T + \lambda_2 \phi_+^S \quad (A3)$$

The second term, ϕ_+^S, couples the orthogonal orbitals into two open-shell singlet pairs. When the orbitals interact initially, they achieve orthogonality by forming bonding–antibonding pairs, and this term serves to introduce ionic contributions. For localized orbitals that are already orthogonal, such as $d\pi_4$ and π_2 in section IIIB, ϕ_+^S need not be of an ionic form. In precise terms, eq 9 of the text is obtained for $\lambda_1 = \lambda_2$, that is

$$\Psi_+ = \phi_+^T + \phi_+^S \quad (A4)$$

Thus, as ϕ_+^S contributes, the total transition-state wave function becomes better represented by eq 9, or

$$\psi_+ = \boxed{\begin{array}{c} (\pi_1 - \pi_3)(\pi_2 - \pi_4) \\ (\pi_1 + \pi_3)(\pi_2 + \pi_4) \end{array}} \quad (A5)$$
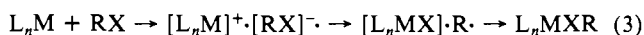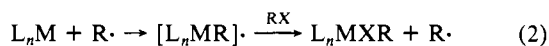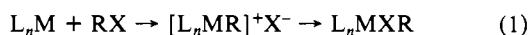
in terms of tableau.

A Mechanistic Study of the Photochemically Initiated Oxidative Addition of Isopropyl Iodide to Dimethyl(1,10-phenanthroline)platinum(II)

Ross H. Hill and Richard J. Puddephatt*

Contribution from the Department of Chemistry, University of Western Ontario, London, Ontario, Canada N6A 5B7. Received June 15, 1984

Abstract: The photochemically initiated oxidative addition of isopropyl iodide to dimethyl(1,10-phenanthroline)platinum(II) (1) has been studied. Irradiation into the lowest energy MLCT band of 1 (λ = 473 nm) leads to iodine atom abstraction from *i*-PrI by the MLCT excited state of 1. This state is shown to have triplet character since the initiation can be effected with use of a triplet sensitizer (benzophenone) and retarded with use of a triplet quencher (pyrene). The initiation is followed by a free radical chain mechanism of oxidative addition, with isopropyl radicals (which may be trapped with use of the radical trap DMPO) as chain carriers. The reaction is retarded in the presence of radical scavengers. The termination step is shown to involve attack of isopropyl radicals at the methyl or 1,10-phenanthroline ligands of 1 and not the expected combination/disproportionation reaction involving two isopropyl radicals. A kinetic analysis of the reaction in the presence and absence of sensitizer, quencher, or scavenger has led to the determination of several of the key rate constants needed to describe quantitatively the chain reaction.

The framework for discussion of mechanisms of oxidative addition of alkyl halides to transition-metal complexes was established over 10 years ago.[1] Three mechanisms, the S_N2 mechanism, with the electron-rich metal center acting as nucleophile, and the free radical chain and nonchain mechanisms have been supported[1,2] (eq 1–3).

$$L_nM + RX \rightarrow [L_nMR]^+X^- \rightarrow L_nMXR \quad (1)$$

$$L_nM + R\cdot \rightarrow [L_nMR]\cdot \xrightarrow{RX} L_nMXR + R\cdot \quad (2)$$

$$L_nM + RX \rightarrow [L_nM]^+\cdot[RX]^-\cdot \rightarrow [L_nMX]\cdot R\cdot \rightarrow L_nMXR \quad (3)$$

A number of techniques have been developed for distinguishing between these mechanisms,[2] but very little is known about the factors which influence whether a reaction will proceed by the free radical chain or nonchain mechanisms or by both mechanisms.[2] This is partly a result of the lack of experimental methods for determining rates of the initiation, propagation, and termination steps of the free radical chain processes. Indeed, even the natures of the initiation and termination steps are obscure in many cases.

The oxidative addition of isopropyl iodide to dimethyl(1,10-phenanthroline)platinum(II) (1) occurs slowly under thermal activation according to eq 4, (N–N ≈ phen).[3]
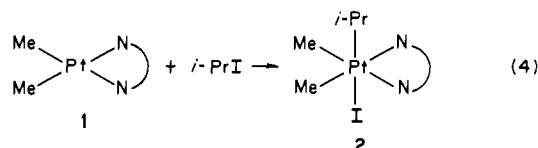
(1) (a) Halpern, J. *Acc. Chem. Res.* **1970**, *3*, 386. (b) Bradley, J. S.; Connor, D. E.; Dolphin, D.; Labinger, J. A.; Osborn, J. A. *J. Am. Chem. Soc.* **1972**, *94*, 4043. (c) Lappert, M. F.; Lednor, P. W. *J. Chem. Soc., Chem. Commun.* **1973**, 948.

(2) (a) Lappert, M. F.; Lednor, P. W. *Adv. Organomet. Chem.* **1976**, *14*, 345. (b) Kochi, J. K. "Organometallic Mechanisms and Catalysis"; Academic: New York, 1978; pp 156–168. (c) Labinger, J. A.; Osborn, J. A.; Coville, N. J. *Inorg. Chem.* **1980**, *19*, 3236. (d) Hall, T. L.; Lappert, M. F.; Lednor, P. W. *J. Chem. Soc., Dalton Trans.* **1980**, 1448.

(3) Ferguson, A.; Parvez, M.; Monaghan, P. K.; Puddephatt, R. J. *J. Chem. Soc., Chem. Commun.* **1983**, 267.

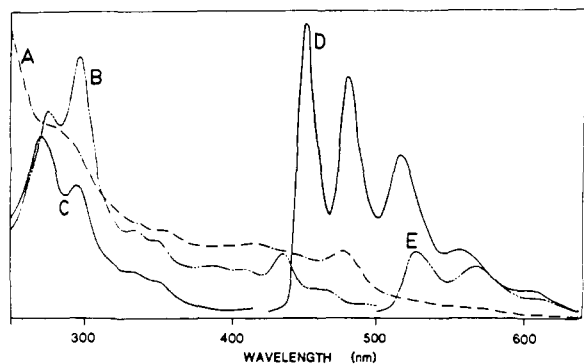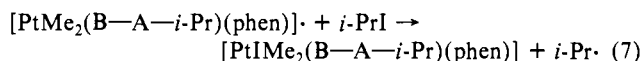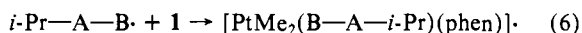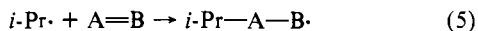**Figure 1.** Spectral properties of [PtMe₂(phen)] showing (A) the absorption spectrum, (B) the excitation spectrum of the emission at 530 nm, (C) the excitation spectrum of the emission at 450 nm, (D) the emission spectrum due to the excitation at 300 nm, and (E) the emission spectrum due to excitation at 450 nm; all spectra are at 77 K in diethyl ether glass.

However, in the presence of unsaturated reagents A=B (O=O or CH₂=CHCN), insertion occurs during the free radical chain process of oxidative addition, according to eq 5–7.[3,4] With use

$$i\text{-Pr} \cdot + A{=}B \rightarrow i\text{-Pr}\text{—}A\text{—}B\cdot \quad (5)$$

$$i\text{-Pr}\text{—}A\text{—}B\cdot + 1 \rightarrow [PtMe_2(B\text{—}A\text{—}i\text{-Pr})(phen)]\cdot \quad (6)$$

$$[PtMe_2(B\text{—}A\text{—}i\text{-Pr})(phen)]\cdot + i\text{-PrI} \rightarrow$$
$$[PtIMe_2(B\text{—}A\text{—}i\text{-Pr})(phen)] + i\text{-Pr}\cdot \quad (7)$$

of a competition method, the second-order rate constant for addition of the isopropyl radical to 1 was estimated to be ∼4 × 10⁻⁶ L mol⁻¹ s⁻¹, but no other rate constants could be determined.[4] It has now been discovered that, at low concentrations of isopropyl iodide (<10⁻² M), the thermal reaction with 1 is negligibly slow but the reaction can still be initiated photochemically. The separation of the photochemical initiation from the thermal propagation and termination steps, studied here for the first time in oxidative addition, leads to an unambiguous characterization of mechanism and to the first determination of the chain length and of quantitative rate data for the initiation, propagation, and termination steps of the chain reaction.

Results

Emission Studies on [PtMe₂(phen)]. The complex 1 gave no detectable emission at room temperature. However, in an ether glass at 77 K, emission is observed. The total emission shown in Figure 1D is a result of excitation at 300 nm. The inset as Figure 1E is the observed emission resulting from excitation at 400 nm. The observation of two emitting states in complexes with similar ligands is not unique but, given the high reactivity of [PtMe₂(phen)], it is difficult to exclude the possibility that the higher energy emission is due to an impurity.[5] Data are given in Table I.

Characterization of Products. Although the reaction of isopropyl iodide with 1 was found to follow the stoichiometry of eq 4 in diffuse daylight,[3] we wished to confirm this under conditions which were clearly photochemical. For this experiment, a solution containing [PtMe₂(phen)], 1 and isopropyl iodide in acetone was degassed and sealed in a Pyrex container with an attached optical

Table I. Absorption and Emission Assignments for [PtMe₂(phen)] and 1,10-Phenonthroline

absorption (10³ cm⁻¹)	assignment	emission (10³ cm⁻¹)	assignment
	[PtMe₂(phen)]		
42.0	IL^a (π–π*)		
35.0	IL^a (π–π*)	22.2	IL^a ^{3}(π–π*)
		20.7	
		19.2	
28.6	MLCT^b (d–π*)		
21.0	MLCT^b (d–π*)	18.9	MLCT ^{3}(d–π*)
		17.6	
		16.3	
	1,10-Phenanthroline		
37.7	(π–π*)		
29.6	(π–π*)	27.4	^{1}(π–π*)
		26.3	
		25.0	
		21.8	^{3}(π–π*)
		20.5	
		19.2	

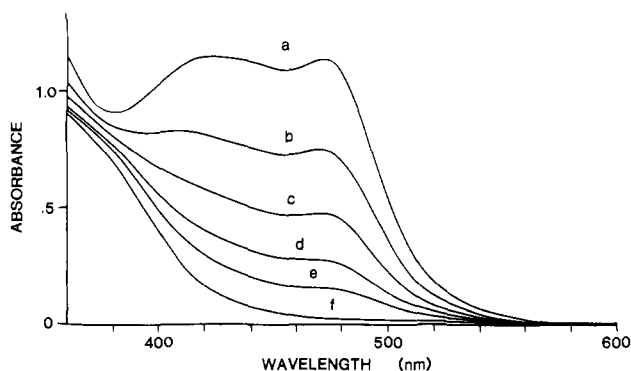^{a} IL = intraligand band. ^{b} MLCT = metal-to-ligand charge-transfer band.

Figure 2. Electronic spectral changes accompanying the 473-nm photolysis of 1 and isopropyl iodide in acetone, with the following number of counts of irradiation: (a) 0; (b) 1; (c) 2; (d) 3; (e) 4; (f) extended irradiation.

cell. Irradiation with the filtered light (pass λ > 420 nm) from a medium-pressure Hg lamp led to decolorization of the initially orange solution. This decay of the absorption in the electronic spectrum, due to a metal-to-ligand charge-transfer band of complex 1,[6] provided a convenient means to follow the extent of reaction. A typical spectral change is shown in Figure 2. The reaction was complete after a 5-min-irradiation time, and the product was found to be pure [PtIMe₂-i-Pr(phen)] (2).

A second experiment was carried out as above except that a free radical inhibitor, 4-methoxyphenol, was added to the solution prior to degassing. In this case the light output from the mercury lamp was not intense enough to promote reaction on a convenient time scale and hence a 150-W high-pressure xenon lamp was used. After 5 min under these conditions, the reaction was near completion and the products were identified as an approximately 1:1 mixture of 2 and [PtI₂Me₂(phen)] (3). This increased formation of 3 indicates that it is formed in the initiation step.

Trapping of Intermediates. Solutions of 1 and isopropyl iodide in benzene were irradiated in the cavity of an ESR spectrometer. Under these conditions, no signal was observed in either fluid or frozen (77 K) solutions. On the addition of DMPO to degassed fluid solutions, an ESR signal (g = 2.0069) appeared as a doublet of triplets, with a_β^H = 21.8 G and a_N = 14.3 G. The parameters are in the range expected for simple alkyl radical trapping (eq 8).[7] Positive identification was made by an independent synthesis

(4) Monaghan, P. K.; Puddephatt, R. J. *Organometallics* **1983**, *2*, 1698.

(5) (a) Fredericks, S. M.; Luong, J. C.; Wrighton, M. S. *J. Am. Chem. Soc.* **1979**, *101*, 7415. (b) Giordano, P. J.; Fredericks, S. M.; Wrighton, M. S.; Morse, D. L. *J. Am. Chem. Soc.* **1978**, *100*, 2257. Preliminary results which suggest that the higher energy emission is not due to an impurity are the following: (1) The results are reproducible with different preparations of 1, and recrystallization of 1 leads to no change in emission. (2) The excitation spectra corresponding to the different emissions [Figure 1C for emission at 450 nm, Figure 1B for emission at 530 nm] are identical in peak position for the region λ = 250–360 nm, but excitation at λ > 360 nm does not give the higher energy emission. (3) The excitation spectra [Figure 1B and 1C] are in qualitative agreement with the absorption spectrum [Figure 1A]. However, it should be noted that the observation of the apparent higher energy emission of 1 at higher energy than the lowest energy absorption band is very unusual.

(6) Chaudhury, N.; Puddephatt, R. J. *J. Organomet. Chem.* **1975**, *84*, 105.

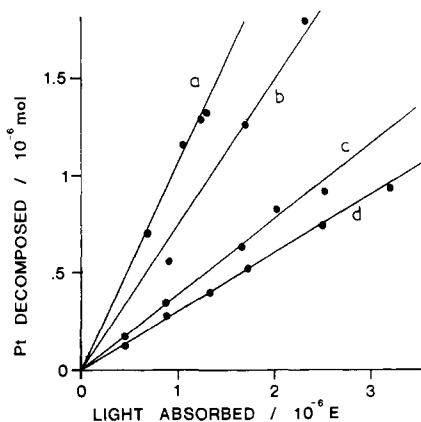(7) Janzen, E. G.; Liu, J. I.-P. *J. Magn. Reson.* **1973**, *9*, 510.

Figure 3. Plot of moles of **1** decomposed vs. einsteins of 473-nm light absorbed for the following isopropyl iodide concentrations: (a) 8.33 × 10^{-3} mol L^{-1}; (b) 5.83 × 10^{-3} mol L^{-1}; (c) 3.27 × 10^{-3} mol L^{-1}; (d) 2.38 × 10^{-3} mol L^{-1}.

Table II. Quantum Yields for Reaction of **1** with Isopropyl Iodide in Acetone

[*i*-PrI], mol L^{-1} × 10^{-3}	Φ	light intensity, einstein count^{-1} × 10^{6}
2.01	0.25	1.0
2.38	0.285	1.0
2.5	0.29	1.0
3.27	0.39	1.0
5.83	0.75	1.0
8.33	1.07	1.0
2.38	0.31	0.5
2.27	0.40	0.5
4.55	0.57	0.5

of the stable radical with R = *i*-Pr by reaction of Hg(*i*-Pr)$_2$ with DMPO. The ESR spectra were identical.

$$(8)$$
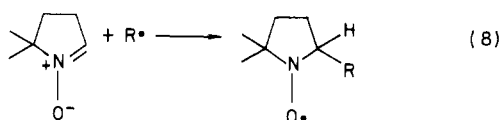
This result indicates that isopropyl radicals are involved in the initiation and/or propagation steps of the reaction.[1,2,8]

Quantum Yields as a Function of Reactant Concentration and of Incident Light Intensity. Rigorously degassed acetone solutions containing **1** and isopropyl iodide were flame sealed in quartz cuvettes. Irradiation at 473 nm was carried out with a standardized light source, and the concentration of **1** was monitored by the decrease in absorbance at 473 nm (see Figure 2). Both the concentration of **1** and the light absorbed by **1** were then calculated. The slope of a graph of moles of **1** reacted vs. einsteins of light absorbed by **1** gives the quantum yield. Plots are shown in Figure 3 for a variety of isopropyl iodide concentrations, and data are given in Table II. In each case an excess of isopropyl iodide was used, such that its concentration remained effectively constant throughout the experiment. In each case, a plot of moles of **1** reacted vs. einsteins of light absorbed was linear over the course of the reaction. This indicates that the quantum yield was unaffected by the concentration of **1**, as the reactions were followed for at least 75% reaction.

As can be seen in Figure 3, the concentration of isopropyl iodide did have an effect on the quantum yield. This variation was studied over the concentration range from 2 × 10^{-3} to 8 × 10^{-3} mol L^{-1}, and a first-order relationship between isopropyl iodide concentration and quantum yield for reaction of **1** was found (Figure 4). It should be noted that, in each case, the reaction
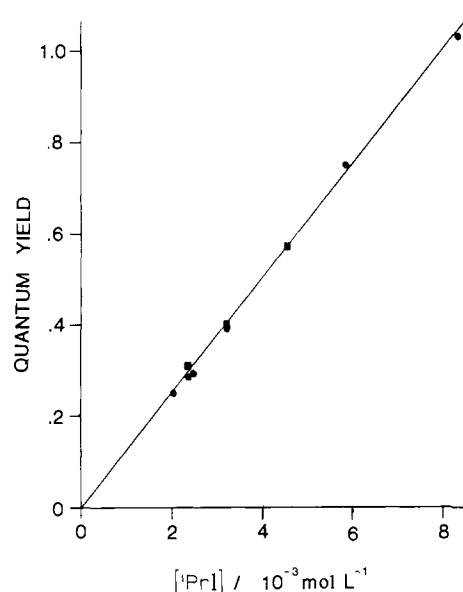
---

(8) The usual cautionary note concerning the high sensitivity of the ESR technique, which permits detection of minor amounts of radicals formed in side reactions, is applicable to this experiment.

Figure 4. Plot of quantum yield for reaction of **1** with isopropyl iodide vs. isopropyl iodide concentration. The incident light intensity is 1.0 × 10^{-6} einstein count^{-1} for circled points and 0.5 × 10^{-6} einstein count^{-1} for squared points.

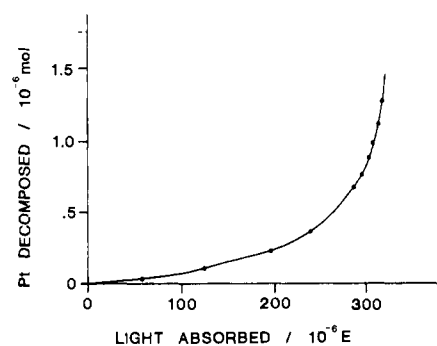**Figure 5.** A plot of moles of [PtMe$_2$(phen)] decomposed vs. einsteins of light absorbed for the reaction of **1** with isopropyl iodide in the presence of oxygen.

was also monitored in the dark in order to confirm that no contribution due to a thermal process was occurring over the time period of the quantum yield measurements.

In each quantum yield measurement, the absorbed light varied with the concentration of **1**. The linear graphs of moles of **1** reacted vs. einsteins of light absorbed hence indicate that there is no dependence of the quantum yield on light intensity. In order to confirm that this observed lack of dependence of the quantum yields on the concentration of **1** and on the light intensity was not an artifact arising from a dependence on both concentration of **1** and light intensity having opposing effects, experiments were carried out in which a 50% neutral density filter was interposed between the light source and the sample. As can be seen in Figure 4 and Table II, this experiment confirmed that there was no dependence of the quantum yield for reaction of **1** with isopropyl iodide on either the concentration of **1** or on the light intensity.

The Effect of Oxygen on the Quantum Yield. One experiment was carried out without degassing the reaction mixture of **1** and isopropyl iodide. In this case a plot of moles of **1** reacted vs. einsteins of light absorbed was not linear, but it had an increasing slope (Figure 5). The initial quantum yield was 1 × 10^{-3} with an isopropyl iodide concentration of 8.33 × 10^{-3} mol L^{-1}. The quantum yield increased greatly over the course of the reaction to a maximum observed value of 3 × 10^{-2}. The linear plots of Figure 3, with reproducible quantum yields, can only be obtained if the solutions are rigorously degassed.

The Effect of Solvent on the Quantum Yields. The quantum yield for decomposition of **1** was measured in benzene and ace-

Table III. The Effect of Inhibitors on Quantum Yield for Reaction of **1** with Isopropyl Iodide

inhibitor	[inhibitor], mol L^{-1}	[i-PrI], mol L^{-1}	Φ initial
benzoquinone	0.88 × 10^{-4}	6.2 × 10^{-3}	0.0024
	1.8 × 10^{-4}	6.2 × 10^{-3}	0.0015
	1.9 × 10^{-4}	5.6 × 10^{-3}	0.0010
	2.2 × 10^{-4}	6.2 × 10^{-3}	0.00066
	9.5 × 10^{-4}	5.6 × 10^{-3}	0.00030
	76 × 10^{-4}	6.2 × 10^{-3}	0.006
4-methoxyphenol	0.65 × 10^{-4}	6.2 × 10^{-3}	0.072
	1.3 × 10^{-4}	6.2 × 10^{-3}	0.049
	2.6 × 10^{-4}	6.2 × 10^{-3}	0.043
	7.0 × 10^{-4}	7.7 × 10^{-3}	0.005
	7.25 × 10^{-4}	6.0 × 10^{-3}	0.0015
	42 × 10^{-4}	6.2 × 10^{-3}	0.00043
hydroquinone	4.4 × 10^{-3}	5.8 × 10^{-3}	0.0045
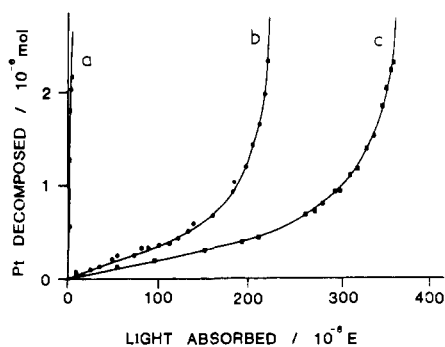
Figure 6. A plot of moles of **1** decomposed vs. einsteins of 473-nm light absorbed for reaction of **1** with isopropyl iodide in the presence of the following concentrations of the free radical inhibitor benzoquinone: (a) 0.0 mol L^{-1}; (b) 8.8 × 10^{-5} mol L^{-1}; (c) 1.9 × 10^{-4} mol L^{-1}.

tonitrile, in order to determine the effect on the quantum yield of changing the solvent polarity at a constant concentration of isopropyl iodide. In acetone, the quantum yield is 0.68 at [i-PrI] = 5.6 × 10^{-3} mol L^{-1} (interpolated value). In benzene, a quantum yield of 0.24 was observed, whereas, in acetonitrile, the quantum yield was 1.8 × 10^{-3} at the same concentration of isopropyl iodide. In acetonitrile, this value was not constant and was found to increase during the course of the reaction. Clearly, there is no correlation of quantum yield with solvent polarity.

The Effect of Free Radical Inhibitors on the Quantum Yields. The effect of free radical scavengers on the quantum yield for reaction of **1** with i-PrI was measured, using degassed solutions. For this study, three inhibitors were used: 4-methoxyphenol, p-benzoquinone, and hydroquinone. All three were found to have a retarding effect on the quantum yield (Table III). A plot of moles of **1** reacted vs. light absorbed is shown in Figure 6 for two different concentrations of p-benzoquinone, showing longer retardation at higher initial p-benzoquinone concentrations. For hydroquinone, although an inhibition was noted, the spectral changes indicated the formation of colored byproducts, and hence these data are of a qualitative nature only.

For p-methoxyphenol the data were again not easily reproducible but the data on *initial* quantum yields for the inhibitor p-benzoquinone were reproducible, although significant changes in Φ also occurred over the course of the reaction (Figure 6). In addition, complications occurred with high concentrations of p-benzoquinone (>10^{-3} M) with formation of colored byproducts.

Triplet Sensitization. The reaction was sensitized by the addition of benzophenone. In this experiment, an acetone solution containing **1**, isopropyl iodide, and benzophenone was degassed and the extent of reaction was followed by monitoring changes in the absorption spectrum in the usual way. The source of light used was such that 80% of the light (λ = 362 nm) was absorbed by the sensitizer and 20% of the light was absorbed directly by **1**. Energy transfer to **1** from benzophenone (E_T = 417 nm, τ_T = 12 μ s; Φ_{ISC} = 1)[9] was assumed to occur with 100% efficiency
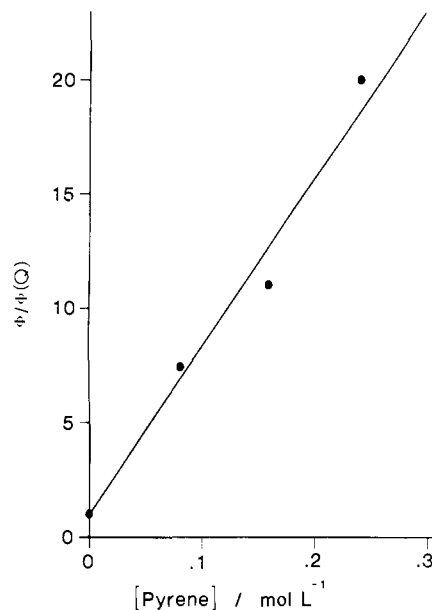
Figure 7. A Stern–Volmer plot of quantum yield in the absence of quencher, Φ, over quantum yield in the presence of quencher, $\Phi(Q)$, vs. the concentration of the quencher pyrene.

from the triplet state with no transfer from the singlet state. Under these conditions, the quantum yield for the reaction from the sensitized triplet state [=moles of **1** reacted/moles of triplet state of **1** produced] was found to be 0.16 ± 0.08. The large uncertainty in quantum yield is due to a portion of the reaction occurring by direct absorption by **1** under the conditions used. A correction for this direct absorption was made but could not be done with great accuracy.

The quantum yield for reaction by direct absorption of 473-nm light by **1** under identical concentration conditions ([i-PrI] = 1.3 × 10^{-3} mol L^{-1}) is 0.16. Hence, the quantum yield for intersystem crossing from the initially excited singlet state of **1** to the reactive triplet state is 1.0 ± 0.3.

Triplet Quenching. The qualitative result of sensitization suggested that the reaction occurred through an excited state of **1**, with mostly triplet character. In order to verify this, the reaction was quenched by pyrene (Q) (E_T = 595 nm, E_S = 372 nm).[9] In these experiments the complex was irradiated at 473 nm. Hence no singlet quenching could occur. The data are presented as a Stern–Volmer plot of quantum yield in the absence of quencher, Φ, divided by quantum yield in the presence of quencher $\Phi(Q)$, vs. the concentration of quencher used, [Q], in Figure 7.

The significance of this straight line plot will be discussed after a kinetic scheme is developed.

Discussion

The Electronic Structure of [PtMe$_2$(phen)]. The absorption spectrum of [PtMe$_2$(phen)] (**1**) has been studied previously. Four distinct bands were assigned.[6] Two high-energy bands, in the regions 36 100 (band 1) and 33 300 cm^{-1} (band 2), were assigned to ligand-localized π–π* transitions. The band positions are similar to the absorptions of free 1,10-phenanthroline and were not dependent on solvent polarity, consistent with the π–π* assignment. The two energies of the additional bands at 28 600 (band 3) and 20 900 cm^{-1} (band 4) in acetone solvent were solvent dependent and hence were assigned as d–π* metal-to-ligand charge-transfer bands.

Before considering the emission from complex **1**, it is useful to review the phosphorescent emission from the free 1,10-

(9) Muron, S. L. "Handbook of Photochemistry"; Marcel Dekker: New York, 1973. The value of k_{diff} = 3 × 10^{10} s^{-1} in acetone is based on a calculation using the modified Debye–Hückel equation, which is known to overestimate k_{diff} for solvents of low viscosity. If k_{diff} is as low as 10^{10} s^{-1}, this would give $k_d \sim$ 1.4 × 10^8 s^{-1} and $k_1 \sim$ 0.5 × 10^7 L mol^{-1} s^{-1}. None of the other rate constants would be affected.

phenanthroline ligand (Table I). The emission is observed in the region 21 800 cm^{-1} with resolved vibrational progression (20 500 and 19 200 cm^{-1}). The emission has been assigned to a $^3(\pi-\pi^*)$ phosphorescence.[10]
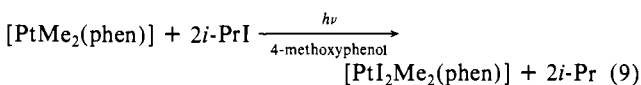
The emission spectrum of **1** consists of two separate structured emissions (Figure 1, Table I). The high-energy emission at 22 300 cm^{-1} is similar to the emission of the free ligand, in both energy and vibrational structure. In view of the possibility that this emission could arise from an impurity, no further discussion is justified at this time.[5,11,12] The lower energy emission at 19 000 cm^{-1} also has vibrational structure. The energy of this band is shifted significantly from the emission for free 1,10-phenanthroline (Table I). A slight overlap with the MLCT absorption band 4 is observed. This low-energy emission is assigned as due to the metal-to-ligand charge-transfer excited state (d → π^*). Previous examples of structured emissions from metal-to-ligand charge-transfer excited states have been observed in complexes of d^6 metal ions. Examples include *cis*-[IrCl$_2$(phen)$_2$]Cl and [Ru(phen)$_3$]I$_2$, in which the emissions were shifted 1100 cm^{-1} and 4600 cm^{-1}, respectively, to low energy from the free ligand and were also assigned as a charge-transfer emission.[13,14] The state from which the low-energy emission from **1** is observed is probably a triplet, and the small shift from the absorption band is explained by the large spin–orbit coupling due to platinum. In some metal complexes such as [IrCl$_2$(phen)$_2$]Cl the spin-orbitally enhanced MLCT singlet–triplet absorption is observed to be superimposed upon the MLCT singlet–singlet absorption.[10] Similar spin–orbit coupling would be expected in **1** and hence the small shift between the lowest energy absorption and emission bands of **1** is compatible with a triplet (d–π^*) emission.

For present purposes, it is important to note that the photochemistry of **1** was studied with use of irradiation at 473 nm and hence the chemistry results only from the lower energy ^{3}(d–π^*) MLCT excited state. Much higher quantum yields were observed with use of irradiation at 362 nm, but interpretation of these results must await a more detailed study of the photophysics of **1**.

The Mechanism of Reaction. The results given above show that the reaction occurs by a free radical chain mechanism with photochemical initiation. The individual steps are discussed below and are summarized in Scheme I.

Initiation. It is clear that, under the conditions used, the reaction of **1** with *i*-PrI is photochemically initiated. The observations that it is possible to quench the reaction with the triplet quencher pyrene and to sensitize the reaction with the triplet sensitizer benzophenone are consistent with the predominantly triplet MLCT, ^{3}(d → π^*) state of **1**, being the reactive state in the initiation. The high value (1.0 ± 0.3) of the quantum yield for intersystem crossing from the ^{1}(d → π^*) to the ^{3}(d → π^*) state is consistent with the large spin–orbit coupling of the platinum atom.[11]
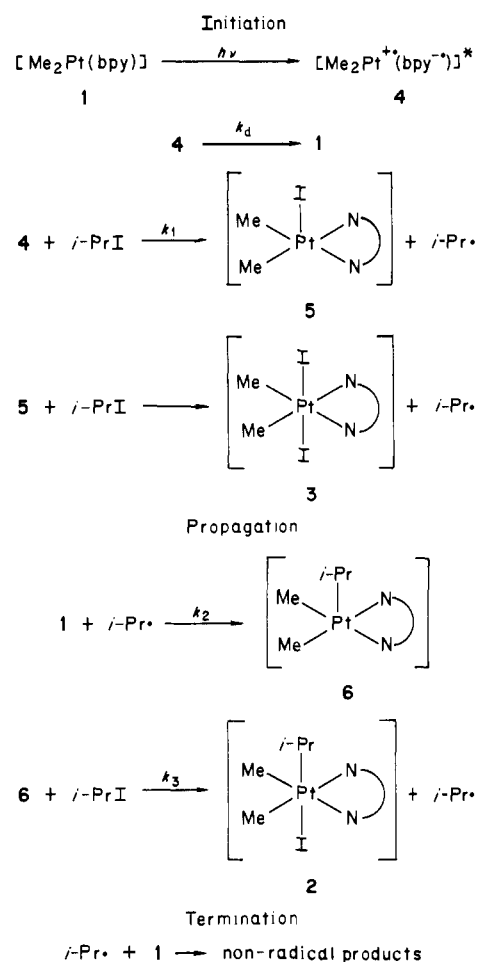
In the presence of the free radical inhibitor 4-methoxyphenol the reaction occurred much less efficiently and produced [PtI$_2$Me$_2$(phen)] (**3**) as in eq 9.

$$[\text{PtMe}_2(\text{phen})] + 2i\text{-PrI} \xrightarrow[\text{4-methoxyphenol}]{h\nu}$$
$$[\text{PtI}_2\text{Me}_2(\text{phen})] + 2i\text{-Pr} \quad (9)$$

The overall initiation sequence, which we propose (Scheme I) to explain the formation of **3**, is analogous to the initiation step proposed for the thermal oxidative addition of BuBr to [Pt(PEt$_3$)$_3$], giving [PtBr$_2$(PEt$_3$)$_2$] and butyl radicals, and to several similar systems.[1,2,15]

Irradiation of **1** produces, with unit efficiency, a triplet excited state, **4**, which may then decay to the ground state with a rate constant k_d or react in a bimolecular fashion with isopropyl iodide

(10) DeArmond, M. K.; Hillis, J. E. *J. Chem. Phys.* **1971**, *54*, 2247.

(11) Forster, L. S. In "Concepts of Inorganic Photochemistry"; Adamson, A. W., Fleischauer, P. D., Eds.; Wiley: New York, 1975.

(12) Carsons, D. H. W.; Crosby, G. A. *J. Mol. Spectrosc.* **1970**, *34*, 113.

(13) Watts, R. J.; Crosby, G. A. *J. Am. Chem. Soc.* **1971**, *93*, 3184.

(14) Klassen, D. M.; Crosby, G. A. *Chem. Phys. Lett.* **1967**, *1*, 127.

(15) Kramer, A. V.; Labinger, J. A.; Bradley, J. S.; Osborn, J. A. *J. Am. Chem. Soc.* **1974**, *96*, 7145.

Scheme I

producing **5** and free isopropyl radicals (Scheme I). The intimate nature of this reaction is not known. However, it may proceed either by direct halogen abstraction from isopropyl iodide by the electron deficient platinum center of **4** or via an initial electron transfer from the reduced phenanthroline ligand of **4** to isopropyl iodide followed by rapid iodide transfer to platinum. Similar mechanisms have been proposed in thermally initiated oxidative additions.[1,2]

The final step, abstraction of a second iodine atom by the platinum(III) center of **5** (Scheme I), is expected to follow rapidly.[1,2,16]

Propagation. The initiation sequence above produces two isopropyl radicals. The trapping of only isopropyl radicals by DMPO, as observed by ESR spectroscopy (eq 8), implicates the isopropyl radical as the radical chain carrier. In order to produce the observed reaction product, **2**, the propagation steps of Scheme I are proposed. A similar sequence of events is believed to be operative in similar thermally initiated reactions (eq 2).[1,2,15]

Termination. The addition of a free radical scavenger was found to reduce the observed quantum yield by as much as a factor of 2 × 10^3 (Table III). This observation indicates a minimum chain length of 1000 (a quantitative estimate of the chain length will be presented later). The products derived from the termination step will therefore represent less than 0.05% of the total reaction products when complex **1** is photolyzed in the presence of *i*-PrI. Because of the small amount of termination products formed, their direct chemical identification was not possible. However, the general nature of the termination reaction could be deduced from a kinetic analysis. It is immediately apparent, from the independence of the quantum yields on the incident light intensity, that the termination step cannot involve the expected bimolecular combination or disproportionation of isopropyl radicals.[17] Instead,

(16) Chen, J. Y.; Kochi, J. K. *J. Am. Chem. Soc.* **1977**, *99*, 1450.

Photochemically Initiated Oxidative Addition

J. Am. Chem. Soc., Vol. 107, No. 5, 1985 1223

the termination step must be first order in concentration of isopropyl radicals.

If a termination sequence given by eq 10, involving an unknown species X, is assumed, an expression for the observed quantum yield, Φ, for reaction of **1** with *i*-PrI can be derived, using the initiation and propagation steps of Scheme I. Assuming steady-state concentrations for the excited platinum complex, **4**, and all radicals (**5, 6**, and *i*-Pr′), the quantum yield should be given by eq 11 (see Appendix for derivation). The chain length is given

$$i\text{-Pr}' + X \rightarrow \text{nonradical products} \qquad (10)$$
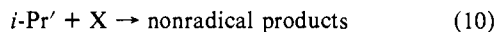
$$\Phi = \frac{k_1[i\text{-PrI}]}{k_d + k_1[i\text{-PrI}]}\left(1 + \frac{2k_2}{k_4}\frac{[1]}{[X]}\right) \qquad (11)$$

by k_2/k_4 and is greater than 1000. Hence, at a constant isopropyl iodide concentration, the quantum yield is expected to be directly proportional to the concentration of **1**. As can be seen from Figure 3, the quantum yield is independent of the concentration of **1**, and this is consistent with eq 11 *only* if X = **1**. The termination must therefore involve reaction of isopropyl radicals with complex **1**, and the expression for the quantum yield is then given by eq 12 (see Appendix) and is independent of the concentration of **1**.

$$\Phi = \frac{k_1[i\text{-PrI}]}{k_d + k_1[i\text{-PrI}]}\left(3 + \frac{2k_2}{k_4}\right) \qquad (12)$$

The termination step may be the result of hydrogen abstraction by isopropyl radical from either the methyl or the 1,10-phenanthroline ligand of **1**, or it may involve addition of the isopropyl radical to the coordinated 1,10-phenanthroline.[18,19] Whatever the intimate details of the process, the resultant platinum complex is removed from the propagation sequence.[20]

From the above, the overall mechanism of Scheme I was deduced.

Determination of Rate Constants. Introduction of a triplet quencher, Q, into the reaction mixture of **1** and isopropyl iodide provides a new decay channel for the excited platinum complex **4** as shown in eq 13. The triplet energy of the quencher pyrene ($E_T = 595$ nm) is lower than the triplet energy of **1**, and we assume that the rate of quenching is diffusion controlled. The rate constant, k_{diff}, for the process is therefore expected to be 3×10^{10} s^{-1} in acetone.[9]

$$4 + Q \rightarrow 1 + {}^3Q^* \qquad (13)$$
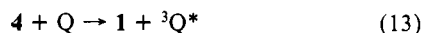
The quantum yield in the absence of quencher, Φ, is given by eq 12. When this new decay channel for **4** is included, a new expression for the quantum yield in the presence of quencher, Φ (Q), can be derived (eq 14). A Stern–Volmer plot (Figure 7) of Φ/Φ(Q) against concentration of pyrene, [Q], will have a slope of $k_{diff}/(k_d + k_1[i\text{-PrI}])$. Since $k_1[i\text{-PrI}] \ll k_d$, the observed slope, 74 ± 9, allows calculation of the rate constant, k_d, to be 4.1 (± 0.5) $\times 10^8$ s^{-1}. The lifetime, τ, of the reactive triplet state, **4**, is given by $(k_d)^{-1} = 2.5$ (± 0.3) $\times 10^{-9}$ s. The short triplet excited-state lifetime of **4** is due to a breakdown in the selection rules, governing triplet–singlet transitions, caused by the large spin–orbit coupling of the platinum metal center. Such short lifetimes for lowest energy triplet states are common when a second- or third-row transition metal is present. For comparison the solution lifetime of emission from a ^{3}MLCT excited state of *cis*-[Ir(phen)$_2$Cl$_2$]Cl is 3.8×10^{-8} s at room temperature.[10]

$$\Phi(Q) = \frac{k_1[i\text{-PrI}]}{k_d + k_1[i\text{-Pr}] + k_{diff}[Q]}\left(3 + \frac{2k_2}{k_4}\right) \qquad (14)$$

(17) Bamford, C. H.; Barb, W. G.; Jenkins, A. D.; Onyon, P. F. "The Kinetics of Vinyl Polymerization by Radical Mechanisms"; Butterworths: London, 1958.

(18) Rollick, K. A.; Kochi, J. K. *J. Am. Chem. Soc.* **1982**, *104*, 1319.

(19) Heilman, W. J.; Rembaun, A.; Swarc, M. *J. Chem. Soc.* **1957**, 1127.

(20) It should be noted that, under the reaction conditions used, a termination step involving decay of **6** to non-radical products would not be consistent with the observed kinetics. A second-order dependence of Φ on [*i*-PrI] would be expected. Hence termination cannot involve initial attack by *i*-Pr· on the platinum center of **1**.
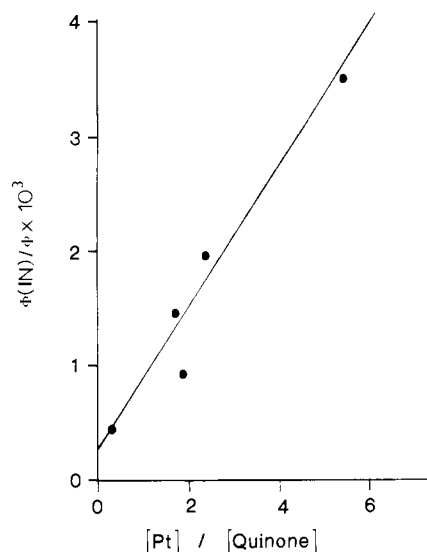

Figure 8. A plot of the ratios of the quantum yields in the presence of inhibitor, Φ(IN), and in the absence of inhibitor, Φ, vs. the ratio of the concentrations of [PtMe$_2$(phen)] and of the free radical inhibitor, benzoquinone.

In the presence of a free radical inhibitor, (IN), the extra kinetic step of eq 15 must be added. An expression for the ratio of the

$$i\text{-Pr}\cdot + \text{IN} \xrightarrow{k_5} i\text{-PrIN} \qquad (15)$$

quantum yield in the presence of inhibitor, Φ(IN), compared to the quantum yield in the absence of inhibitor, Φ, as shown in eq 16 can then be derived (Appendix). As can be seen from eq 16

$$\frac{\Phi(\text{IN})}{\Phi} = \frac{k_4}{2k_2} + \frac{k_4[1]}{k_5[\text{IN}]} \qquad (16)$$

a plot of Φ(IN)/Φ vs. [1]/[IN] is expected to be linear. Such a plot is shown in Figure 8, using the inhibitor *p*-benzoquinone. From eq 16 we can see that the slope of this plot, $6 \pm 1 \times 10^{-4}$, corresponds to k_4/k_5 and that the intercept, $3 \pm 1 \times 10^{-4}$, corresponds to $k_4/2k_2$.[21]

It should be noted that the average chain length is given by the ratio of the rate of propagation, $k_2[1][i\text{-Pr}\cdot]$, to the rate of termination, $k_4[1][i\text{-Pr}\cdot]$, or k_2/k_4. Hence the chain length is calculated to be 1700 (± 700).

Finally, the quantum yield, Φ, in the absence of both quencher and inhibitor, is given by eq 12. It should be noted that k_d, 4.1 (± 0.5) $\times 10^8$ s^{-1}, is much larger than $k_1[i\text{-PrI}]$, as is indicated by the observed linearity of a plot of Φ vs. concentration of isopropyl iodide (Figure 3). The slope of this graph, 123 $\pm$ 5, corresponds to the quantity $k_1(3 + 2k_2/k_4)/k_d$. Using the value for k_d obtained from triplet quenching experiments and the value of $2k_2/k_4$ obtained from free radical inhibition experiments, we can arrive at a value of $k_1 = 1.5$ (± 0.7) $\times 10^7$ L mol^{-1} s^{-1}. The original assumption, that k_d is greater than $k_1[i\text{-PrI}]$, can now be tested. The maximum concentration of isopropyl iodide used was 10^{-2} mol L^{-1}. Hence $k_1[i\text{-PrI}]$ has a maximum value of 2.2 $\times 10^5$ s^{-1}, much less than the value of 4.1 (± 0.5) $\times 10^8$ s^{-1} observed for k_d.

Although we now have absolute values for k_1 and k_d, the remaining rate constants k_2, k_4, and k_5 can only be obtained as relative values. In order to determine absolute values for k_2 and k_4, we must assume a value for k_5, the rate constant for isopropyl radical attack at *p*-benzoquinone. The only estimate of a rate constant for free radical attack on *p*-benzoquinone, 2.0 (± 1) $\times$

(21) The linearity observed in Figure 8 gives further confirmation that termination rate in the absence of inhibitor is given by $k_4[i\text{-Pr}][1]$ as deduced. Care must be taken in choosing quenchers and inhibitors in these reactions, since many reagents could act as *both* quencher *and* inhibitor. It is possible that O$_2$ acts in this way.

10^7 L mol^{-1} s^{-1}, was for attack by the 5-hexenyl radical at 69 °C.[22] Assuming a temperature dependence such that the rate at 25 °C is 1.0×10^7 L mol^{-1} s^{-1}, consistent with a variety of systems involving attack by the 5-hexenyl radical on other molecules,[22] we can now calculate k_2 and k_4. It is found that $k_2 = 1.0$ (± 0.2) $\times 10^7$ L mol^{-1} s^{-1} and $k_4 = 6$ (± 3) $\times 10^3$ L mol^{-1} s^{-1}. It should be noted that the errors given for the values k_2 and k_4 are estimated by using the assumption that the value of $k_5 = 1.0 \times 10^7$ L mol^{-1} s^{-1} has no associated error. The actual error on the values of k_2 and k_4 are presumably much larger.

In a previous study, based on a competition to isopropyl radicals between complex 1 and acrylonitrile, the ratio of rate constants for attack of *i*-Pr· at these centers was found to be 20 ± 10.[4] If the rate constant for attack by isopropyl radicals on acrylonitrile is the same as that for the 5-hexenyl radical (5.3×10^5 L mol^{-1} s^{-1} at 25 °C),[22] then the rate constant, k_2, for attack of *i*-Pr· at 1 is 1.1 (± 0.5) $\times 10^7$ mol^{-1} s^{-1}. This is in excellent agreement with the value for k_2 calculated here by a different method and lends strong support to our interpretation of the mechanism and to the kinetic analysis developed from this.[24]

Conclusions

It has been shown that the photochemical initiation of reaction between isopropyl iodide and [PtMe$_2$(phen)] occurs from a state with primarily triplet character and involves overall iodine atom abstraction from isopropyl iodide. The separation of this photochemical initiation from the subsequent thermal propagation and termination reactions (Scheme I) of the chain reaction is shown to be particularly valuable, since it has permitted a kinetic analysis to be completed and the rate constants for several of the elementary steps to be determined for the first time.

Experimental Section

[PtMe$_2$(phen)] and Hg-*i*-Pr$_2$ were obtained by published procedures[6,27] and identified by their ^{1}H NMR spectra. [PtMe$_2$(phen)] was purified by recrystallization from acetone.

Spectroscopic grade acetone and "gold label" acetonitrile were used without further purification.

Room-temperature absorption spectra were measured on a Cary-118 spectrophotometer. Low-temperature absorption spectra were measured on a Perkin-Elmer Coleman 124 spectrophotometer.

Emission spectra were recorded with a Perkin-Elmer MPF-4 spectrophotometer with a phosphorescence accessory, from which the rotating cam was removed.

The emission spectra were corrected for detector sensitivity, and the excitation spectra were corrected for the spectral distribution of the lamp. In a typical experiment a solution of [PtMe$_2$(phen)] (1×10^{-4} mol L^{-1}) in Et$_2$O (0.5 mL) in a 5-mm quartz tube was cooled to 77 K. The measurements were conducted on the glass produced. The experiment

was repeated by using different samples of [PtMe$_2$(phen)] and also by extracting a sample of [PtMe$_2$(phen)] (0.05 g) into ether. All such samples gave reproducible spectra.

Preparation of [PtIMe$_2$-*i*-Pr(phen)]. A solution (15 mL) of [PtMe$_2$(phen)] (5×10^{-3} mol L^{-1}) and isopropyl iodide (5.2×10^{-3} mol L^{-3}) was degassed in acetone. The sample was irradiated with the light output from a medium-pressure mercury lamp, filtered through both H$_2$O and a C-370 filter. The sample was placed 15 cm from the light source. The reaction was monitored by following the decrease in absorbance at 473 nm. At the end of the reaction (≈ 5 min), the vessel was opened and the solvent was evaporated on a rotary evaporator. The ^{1}H NMR spectrum was then obtained on the product and found to be identical with the spectrum of an authentic sample.[3] NMR (CD$_2$Cl$_2$): δ 1.58 (s, ^2J(PtH) = 72 Hz, PtCH$_3$), 1.81 (septet, ^3J(HH) = 6.5 Hz, CHMe$_2$), 0.16 (d, ^3J(HH) = 6.5 Hz, ^3J(PtH) = 65 Hz, C$_H$Me$_2$).

A similar experiment was carried out in which *p*-methoxyphenol (2.4 $\times 10^{-2}$ mol L^{-1}) was added prior to degassing the solution. In this case, the output from the Hg lamp used previously was insufficient to induce reaction and hence a 150 W high-pressure xenon lamp was used. Again, the output was filtered through H$_2$O and a Corning 0-52 filter. The product mixture, as identified by the ^{1}H NMR spectrum, consisted of an approximately 1:1 mixture of [PtIMe$_2$-*i*-Pr(phen)] and [PtI$_2$Me$_2$-(phen)][3] {NMR (CD$_2$Cl$_2$): δ 2.53 (s, ^2J(PtH) = 74 Hz, PtMe)}.

ESR Spectra. A degassed solution (1.0 mL) of [PtMe$_2$(phen)] (0.0085 g) and isopropyl iodide (0.02 mL) in benzene (10 mL) was irradiated in the cavity of the ESR spectrometer; no signal was observed. The experiment was repeated with DMPO (0.1 mL) added and an intense ESR signal was observed. When irradiation was halted, the signal decayed slowly and reappeared on further irradiation ($g = 2.0063$; peak width = 1.6 G; hyperfine splitting, $a_\beta^H = 21.8$ G, $a_N = 14.3$ G). An identical signal was obtained upon warming a degassed solution of Hg(*i*-Pr)$_2$ and DMPO in benzene.

Quantum Yield Determinations. The 473-nm band of the Jasco CRM-FA spectroirradiator was used and calibrated by using ferrioxalate actinometry.

In a typical experiment stock solutions of [PtMe$_2$(phen)] and isopropyl iodide in acetone were prepared. Aliquots of these were mixed and 5.0 mL of the resultant solution concentration of [PtMe$_2$(phen)] = 6.6×10^{-4} M; a 5.83×10^{-3} M concentration of isopropyl iodide was degassed. A plot of moles of [PtMe$_2$(phen)] reacted vs. light absorbed was made. This was found to be linear (Figure 3), and the quantum yield was obtained from the slope.

This experiment was repeated with a variety of isopropyl iodide concentrations, and the quantum yields are reported in Table II.

Quantum yields were also determined in the presence of the free radical scavengers, benzoquinone and 4-methoxyphenol. In a typical experiment a solution (4.0 mL) containing [PtMe$_2$(phen)] (6.54×10^{-4} mol L^{-1}), isopropyl iodide (6.2×10^{-3} mol L^{-1}), and benzoquinone (2.2×10^{-4} mol L^{-1}) was degassed and flame sealed into a quartz cuvette. The solution was then irradiated, and the extent of reaction was determined by monitoring the optical density at 473 nm. A plot of moles of [PtMe$_2$(phen)] reacted vs. einsteins of light absorbed was then constructed (Figure 6). The quantum yield was calculated from the initial slope of this line and found to be 6.6×10^{-4}. The quantum yields are reported in Table III for a variety of concentrations of both benzoquinone and 4-methoxyphenol.

Triplet quenching experiments were also undertaken by using the known triplet quencher pyrene.[9] In a typical experiment a solution of [PtMe$_2$(phen)] (1.37×10^{-4} mol L^{-1}), isopropyl iodide (1.30×10^{-3} mol L^{-1}), and pyrene (8.0×10^{-2} mol L^{-1}) in acetone (5 mL) was degassed and flame sealed in a quartz cuvette. The solution was then irradiated at 473 nm and the extent of reaction was determined by monitoring the absorbance at 473 nm. For this experiment, the light source was not calibrated and hence plots of moles of [PtMe$_2$(phen)] reacted vs. counts of irradiation was made. A blank experiment was carried out, with no pyrene present, and analyzed in the same manner. The slope of the plot for the blank experiment divided by the slope in the presence of pyrene gave rise to a ratio $\Phi/\Phi(Q)$ of 7.2. This experiment was repeated with different pyrene concentrations of 0.159 and 0.239 mol L^{-1} to yield ratios $\Phi/\Phi(Q)$ of 11 and 20, respectively.

The reaction was also triplet sensitized with benzophenone.[9] In this experiment, a solution of [PtMe$_2$(phen)] (1.37×10^{-4} mol L^{-1}), isopropyl iodide (1.30×10^{-3} mol L^{-1}), and benzophenone (0.02 mol L^{-1}) in acetone (5 mL) was degassed and flame sealed. The irradiation was then carried out with use of the 362-nm band of the light source. The observed quantum yield, calculated in the usual way, was found to be 0.68. The quantum yield was then measured under identical conditions in the absence of benzophenone and found to be 2.6.[28] Under the concentration

(22) Citterio, A.; Arnoldi, A.; Minisci, F. *J. Org. Chem.* **1979**, *44*, 2674.

(23) It is possible to check that termination by combination/disproportionation of *i*-Pr· radicals is slow with respect to the termination step of Scheme I. The maximum steady-state concentration of *i*-Pr· radicals under our conditions is calculated to be $\sim 6 \times 10^{-9}$ mol L^{-1}, and the mean rate of termination according to Scheme I is then $\sim 1.2 \times 10^{-8}$ mol L^{-1} s^{-1}. If we take $k = 10^{8.6 \pm 1.1}$ L mol^{-1} s^{-1} for combination/disproportionation of *i*-Pr· radicals in the gas phase[24] and assume that the decrease from gas phase to acetone solution is by a factor of 10, as found for Me' radical combination,[25] we estimate $k \sim 10^{7.6}$ L mol^{-1} s^{-1} in acetone solution. The rate of loss of *i*-Pr radicals by combination/disproportionation of *i*-Pr· radicals is then $\sim 1.8 \times 10^{-9}$ mol L^{-1} s^{-1}. The errors are too high for this to be considered a proof, but it clearly is reasonable that this rate is low compared to the proposed step (Scheme I). Possibly at high light intensity this might be competitive as a termination step.

(24) Benson, S. W.; Hiatt, R. *Int. J. Chem. Kinet.* **1972**, *4*, 151.

(25) (a) Mickwich, D.; Turkevich, J. *J. Phys. Chem.* **1968**, *72*, 3703. (b) Pryor, W. A.; Platt, P. K. *J. Am. Chem. Soc.* **1963**, *85*, 1496. (c) Nonhebel, D. C.; Walton, J. C. "Free Radical Chemistry"; Cambridge, U. P.: Cambridge, 1974. (d) Marshall, R. M.; Purnell, J. H. *J. Chem. Soc., Chem. Commun.* **1972**, 764.

(26) The value for $k_2 = 4 \times 10^6$ L mol^{-1} s^{-1} was calculated by using an interpolated rate constant for attack of Et' on CH$_2$=CHCN in the gas phase and assuming this was the same for the *i*-Pr· radical in acetone solution. For consistency, we use the value for the 1-hexenyl radical here but note that the values are consistent within the error limits quoted.

(27) Dessy, R. E.; Flautt, T. J.; Jaffe, H. J.; Reynolds, G. F. *J. Chem. Phys.* **1959**, *30*, 1422.

conditions used, 20% of the light was absorbed directly by [PtMe$_2$-(phen)]. Hence, correcting for this, the quantum yield for reaction from the sensitized triplet state is 0.15.

Appendix

Derivation of Kinetic Scheme. The following expressions can be written, based on the mechanism of Scheme I, for decay or formation of **1**, **4**, **6**, and i-Pr.

$$-d[\mathbf{1}]/dt = I_{abs} - k_d[\mathbf{4}] + k_2[i\text{-Pr}][\mathbf{1}] + k_4[i\text{-Pr}][\mathbf{1}]$$

$$d[\mathbf{4}]/dt = I_{abs} - k_d[\mathbf{4}] - k_1[\mathbf{4}][i\text{-PrI}]$$

$$d[i\text{-Pr}]/dT = 2k_1[\mathbf{4}][i\text{-PrI}] - k_4[\mathbf{1}][i\text{-Pr}]$$

$$d[\mathbf{6}]/dt = k_2[\mathbf{1}][i\text{-Pr}] - k_3[\mathbf{6}][i\text{-PrI}]$$

Assuming the steady-state approximation for [**4**], [**6**], and [i-Pr] gives

$$[\mathbf{4}] = I_{abs}/\{k_d + k_i[i\text{-PrI}]\}$$

$$[\mathbf{6}] = k_2[\mathbf{1}][i\text{-Pr}]/k_3[i\text{-PrI}]$$

$$[i\text{-Pr}] = 2k_1[\mathbf{4}][i\text{-PrI}]/k_4[\mathbf{1}]$$

$$\therefore -d[\mathbf{1}]/dt = I_{abs} - k_d I_{abs}/\{k_d + k_1[i\text{-PrI}]\} +$$
$$2k_1 k_2 I_{abs}[i\text{-PrI}]/k_4\{k_d + k_1[i\text{-PrI}]\} + 2k_1 I_{abs}[i\text{-PrI}]/\{k_d + k_1[i\text{-PrI}]\}$$

$$\therefore \Phi = \frac{-d[\mathbf{1}]/dt}{I_{abs}} = \frac{k_1[i\text{-PrI}]\{3 + 2k_2/k_4\}}{\{k_d + k_1[i\text{-PrI}]\}}$$

---

(28) Note the much higher quantum yield when 362-nm irradiation is used. For comparison, the quantum yield with 473-nm irradiation under these concentration conditions was 0.16. This must be due to more efficient initiation from the upper excited state of **1**, presumably the state which gives the higher energy emission discussed earlier. This higher state is inaccessible with 473-nm irradiation, and we have not studied the upper excited state photochemistry further.

The kinetics in the presence of a quencher, Q, must include the extra step of eq 13. The following modified expressions result (k_{diff} = diffusion controlled rate constant)

$$-d[\mathbf{1}]/dt =$$
$$I_{abs} - k_d[\mathbf{4}] + k_2[i\text{-Pr}][\mathbf{1}] + k_4[i\text{-Pr}][\mathbf{1}] - k_{diff}[Q][\mathbf{1}]$$

$$d[\mathbf{4}]/dt = I_{abs} - k_d[\mathbf{4}] - k_1[\mathbf{4}][i\text{-PrI}] - k_{diff}[Q][\mathbf{1}]$$

The quantum yield in the presence of quencher, Φ(Q), is then

$$\Phi(Q) = \frac{k_1[i\text{-PrI}]\{3 + 2k_2/k_4\}}{\{k_d + k_1[i\text{-PrI}] + k_{diff}[Q]\}}$$

The kinetics in the presence of inhibitor, IN, must include the extra step of eq 15 and the following modified expression results.

$$d[i\text{-Pr}]/dt = 2k_1[\mathbf{4}][i\text{-PrI}] - k_4[\mathbf{1}][i\text{-Pr}] - k_5[\text{IN}][i\text{-Pr}]$$

A similar treatment gives the expression for the quantum yield in the presence of inhibitor, Φ(IN), as

$$\Phi(\text{IN}) = \frac{k_1[i\text{-PrI}]\{3[\mathbf{1}] + 2k_2[\mathbf{1}]/k_4 + k_5[\text{IN}]/k_4\}}{\{k_d + k_1[i\text{-PrI}]\}\{k_4[\mathbf{1}] + k_5[\text{IN}]\}}$$

$$\frac{\Phi(\text{IN})}{\Phi} = \frac{\{3[\mathbf{1}] + 2k_2[\mathbf{1}]/k_4 + k_5[\text{IN}]/k_4\}}{\{k_4[\mathbf{1}] + k_5[\text{IN}]\}\{3 + 2k_2/k_4\}}$$

Under the conditions used in these experiments, the chain length, $k_2/k_4 \gg 3$, and termination was mostly due to reaction with inhibitor, so that $k_5[\text{IN}] \gg k_4[\text{Pt}]$. Since $k_2 \gg k_4$, the expression simplifies to

$$\frac{\Phi(\text{IN})}{\Phi} = \frac{k_4}{2k_2} + \frac{k_4[\mathbf{1}]}{k_5[\text{IN}]}$$